

## THE METHODOLOGY OF INVESTIGATION ON RED- AND BLACK-FIGURED POTTERY OF UNKNOWN PROVENANCE

Natalia ROVELLA\*, Valeria COMITE, Michela RICCA

Department of Biology, Ecology and Earth Sciences, University of Calabria,  
Via Pietro Bucci, Arcavacata di Rende (CS), Italy

---

### *Abstract*

*This contribution is concerned with the archaeometric study of seven red- and black-figured potteries, kindly provided by the Carabinieri Corps for Protection of Cultural Heritage, Cosenza Unit (Calabria, Italy). The study was aimed to establish the authenticity of the archaeological artifacts and for this purpose an analytical approach, based on mineralogical and geochemical investigations, was applied. Petrographic analysis (OM), scanning electron microscopy (SEM) coupled with EDS microanalysis and X-ray diffraction (XRD) studies were carried out with the aim of identifying technological features, microstructure and to obtain information on the technological features of each sample. Finally, Fourier transform infrared spectroscopy (FT-IR) was used to detect possible surface coatings.*

**Keywords:** *Archaeological potteries; red- and black-figured; archaeometry; authenticity*

---

### **Introduction**

Studies on the authentication, provenance and technological details of the manufacture of pottery can yield important archaeological information allowing both the determination of trading patterns, and information about the degradation phenomena [1-5]. In addition, a proper archaeometric investigation can help in the detection of modern forgeries or ancient copies of original works. The latter represents an important research topic in the field of cultural heritage [6].

This paper presents data on the characterization of seven red- and black-figured potteries provided by the Cosenza Unit, Carabinieri Corps for Protection of Cultural Heritage (Calabria, Italy). The artefacts were found and seized by the Corps. These objects were identified by an archaeological point of view and studied by means of a campaign of archaeometric analysis to evaluate their manufacture and possibly their authenticity.

Red- and black-figured potteries are among the highest artistic and technological achievements of ancient Greek handicrafts. They were decorated with a background application of a fine-grained clay slurry of appropriate composition, which could vitrify in a shorter time and at a lower temperature than the clay used for the body [7-11].

---

\* Corresponding author: [natalia.rovella@unical.it](mailto:natalia.rovella@unical.it)

The techniques used to produce Attic ceramics and the chemical composition of the black paint has long interested scholars [12]. The pieces underwent only one firing process, consisting of a sequence of oxidizing and reducing steps. Proper control of time and temperature was necessary to ensure vitrification of the fine-grained clay during reduction (i.e., while it was black, owing to the formation of iron (II) compounds), so that it maintained its color in the later oxidizing conditions [11].

The complementary use of archaeometric methodologies provided both information about the compositional features of the analyzed items and objective confirmation of their authenticity.

## Materials and Methods

### Sampling

The seven red- and black-figured potteries were hidden underground and were taken away during a requisition in an unknown location between Calabria and Sicily (Southern Italy). From an archaeological point of view the artefacts (Fig. 1) were described such as:

- *Lekanis*, IV century B.C. (sample L11);
- *Pelike* red-figured technique, Italiot production, late IV century B.C. (sample PE46);
- Crater to volute, IV-III centuries B.C. (sample CV48);
- *Bombylios* black-figured technique, IV- III centuries B.C. (sample B81);
- Crater to bell red-figured technique, Italiot production, IV century B.C. (sample CB96);
- *Phiale* red-figured technique, Italiot production, late IV century B.C. (sample P100);
- *Oinochoe* red-figured technique, Italiot production, late IV century B.C. (sample O115).

Micro-samples were collected in different hidden areas from the artefacts preserving the aesthetic of the objects; they consist both of ceramic body and black gloss.

A list of examined samples along with sampling point and a short description is reported in Table 1.

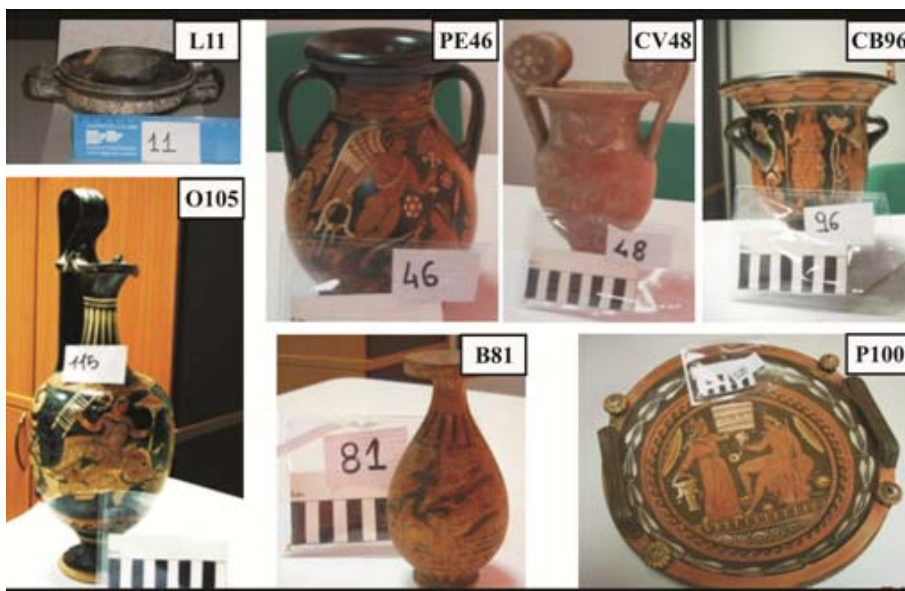


Fig.1. Sampled archaeological pottery.

**Table 1.** Description of the sampling points of the pottery

Sample	Sampling point	Description
L11	Outer edge	Ceramic body and black gloss
PE46	Based outer edge of the vase	Ceramic body and black gloss
CV48	Based outer edge of the crater	Ceramic body and black gloss
B81	Based outer edge of the vase	Ceramic body and black gloss
CB96	Based outer edge of the vase	Ceramic body and black gloss
P100	Outer edge	Ceramic body and black gloss
O115	Based outer edge of the vase	Ceramic body and black gloss

### *Analytical methods*

Minero-petrographic and micro-chemical investigations were carried out for an exhaustive characterization of the samples and to gain information about their authenticity. Analyses performed include:

- Thin-section observations, carried out through a Zeiss Axioskop 40 polarizing microscope, allowed the definition of textural and compositional features of the ceramic pastes.
- X-ray powder diffraction analyses (XRPD) were performed on a D8 Advance Bruker diffractometer with CuK $\alpha$  radiation, using the following working conditions: step-size of 0.02° 2 $\theta$ , step time of 2s/step, analytical range 3-65°. The goal is to identify the constituent phases and to estimate roughly the firing temperature of bricks.
- Scanning electron microscopy (SEM 360 Cambridge Instruments Stereoscan) equipped with an EDAX Philips microanalysis working in energy dispersive spectrometry (EDS) allowed to investigate the microstructure and to obtain information on the major element compositions of the samples. Analyses were carried out with an acceleration voltage of 20 kV and under high vacuum conditions (10<sup>-5</sup> mbar pressure).
- FT-IR investigations were performed by a Perkin Elmer Spectrum 100 equipped with an attenuated total reflectance (ATR) accessory. Infrared spectra were recorded in ATR mode, in the range of 500-4000cm<sup>-1</sup> at a resolution of 4cm<sup>-1</sup> in order to detect possible surface coatings.

## **Results**

### *Petrographic analysis*

Petrographic thin-section investigation was performed by polarizing microscopy, according to *Whitbread* [13], which facilitates detailed characterization of microstructure, groundmass, and inclusions. For each sample all the textural features observed are described below (Fig. 2).

Sample L11 is characterized by a paste with a grain size ranging from very fine (0.01-0.1mm) to fine (0.1-1mm) and by a microstructure with meso- (0.05-0.5mm) and macro-voids (0.5-2mm) (~20%). The groundmass is mainly homogeneous with a color that in plane polar light (PPL) varies from light-brown to brown. The optical activity varies from being absent to low and amorphous concentration features (Acf), consisting of impregnated portions, can be observed. As regards the composition, inclusions, from sub-angular to acicular, show a moderately homogeneous distribution and being single- and double-spaced. They mainly consist of quartz, feldspars, calcite and micas, which rarely exhibit a preferred orientation. In addition Fe-oxides were observed. The c:f (coarse:fine) ratio is ~ 40:60.

Sample PE46 shows a paste type very fine (0.01-0.1mm) to medium (1-5mm) grained and a very compact microstructure in which just a macro-void of 2mm diameter is observed. The groundmass is quite well homogeneous with a brownish color (PPL). The optical activity is high and amorphous concentration features (Acf) of pure type can be observed. Inclusions, from

sub-angular to acicular, consist of quartz, feldspars micas and rare Fe-oxides. They were generally double-spaced and no preferred orientations were observed. The c:f ratio is ~ 40:60.

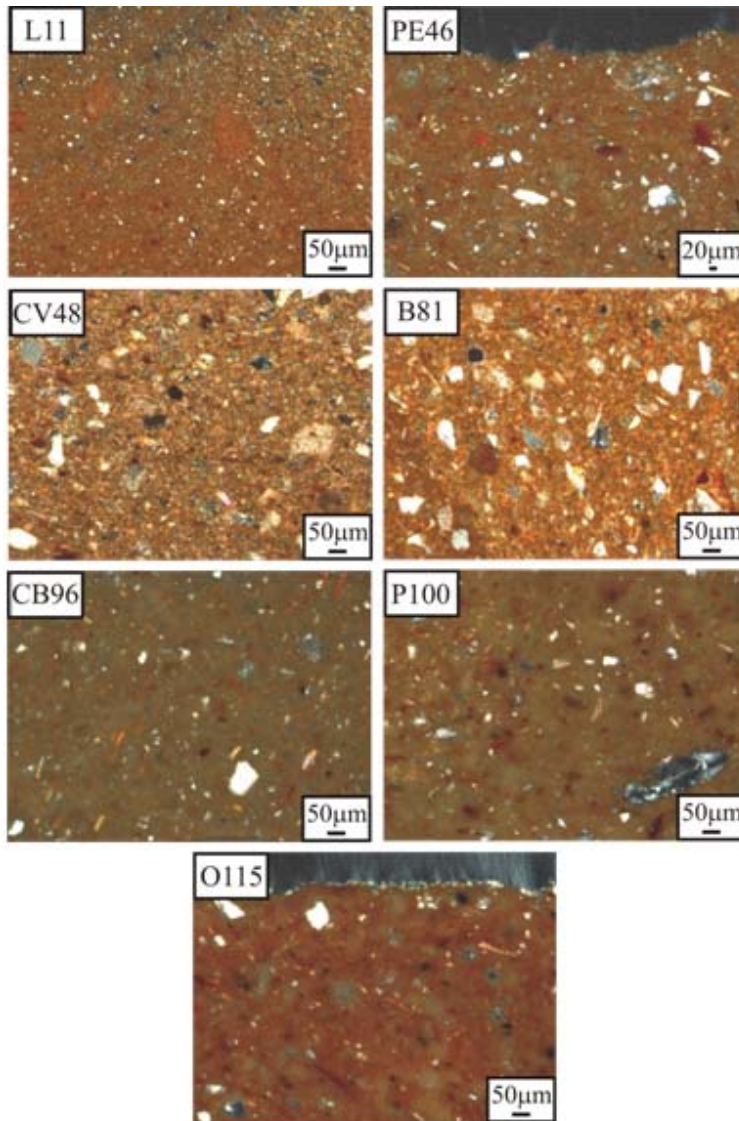


**Fig. 2.** Photomicrographs of pottery samples.

Sample CV48 displays a bimodal distribution, with grain size ranging from medium to coarse (< 5mm) and by a microstructure with macro (0.5-2mm) and mega-voids (> 2mm) (~20%). The groundmass is quite well homogeneous with a color that in plane polar light (PPL) is yellowish. The optical activity is absent and amorphous concentration features (Acf), consisting of impregnate portions, can be observed. Inclusions, single-spaced, from sub-rectangular, sub-triangular to acicular shape, consist of quartz, feldspars, calcite and rare Fe-oxides. No preferred orientations were observed. The c:f (coarse:fine) ratio is ~ 40:60.

Sample B81 is characterized by a fine-medium grain size (0.01-5mm) and by a microstructure mainly consisting of holes and vesicles which dimensions varying from macro-

(0.5-2mm) to mega (> 2mm) (~30%). The groundmass is homogeneous with a color that in plane polar light (PPL) is brownish. The optical activity is high and amorphous concentration features (Acf) consisting of impregnate portions, can be observed. Inclusions, from sub-angular to acicular, mainly consist of quartz, feldspars, and micas. Also, calcite and rare Fe-oxides are observed. They show a single- and double-space distribution. No preferred orientations were observed. The c:f (coarse:fine) ratio is ~ 40:60.

Sample CB96 shows a bimodal distribution with grain size ranging from fine (0.01-0.1mm) to medium (1-5mm) and a very compact microstructure. The groundmass is homogeneous with a color that in plane polar light (PPL) varying from brown to brownish. The optical activity is absent and amorphous concentration features (Acf) of pure type can be observed. Regarding the composition, inclusions, from sub-angular to acicular, mainly consist of quartz, feldspars, Fe-oxides and micas. The latter exhibit a preferred orientation. In addition grains display a single- and double-space distribution. The c:f (coarse:fine) ratio is ~ 40:60.

Sample P100 is characterized by a grain size ranging from fine (0.01-0.1mm) to medium (1-5mm) and a very compact microstructure mainly consisting of mega-voids with diameter greater than 2mm (~10%). The groundmass is quite well homogeneous with a color that in plane polar light (PPL) varying from brown to dark-brown. The optical activity is absent and amorphous concentration features (Acf) of impregnate type can be observed. Inclusions, from sub-angular to acicular, predominantly consist of quartz, feldspars, Fe-oxides, calcite and micas. Grains do not exhibit a preferred orientation and their distribution range from single- to double-space. The c:f (coarse:fine) ratio is ~ 40:60.

Sample O115 shows a fine grain size (0.1-1mm) and a microstructure in which voids ranging from meso- (0.05-0.5mm) to macro- (0.5-2mm) (~20%). The groundmass is homogeneous with a color that in plane polar light (PPL) is reddish. The optical activity is absent and amorphous concentration features (Acf) of impregnate type can be observed. As regards the composition, inclusions, from sub-angular to acicular, show a moderately homogeneous distribution. They mainly consist of quartz, feldspars, Fe-oxides and micas. The latter rarely exhibit a preferred orientation. Also, grains display a single- and double-space distribution. The c:f (coarse:fine) ratio is ~ 30:70.

**XRD analyses**

XRD was used to determine mineralogical composition of the ceramic body and to evaluate firing temperatures [14]. Identified mineralogical phases are listed in Table 2.

XRD analysis shows a heterogeneous composition in all samples thanks to the presence of predominant quartz and subordinated feldspar, hematite, diopside and clay minerals.

In addition, L11, CV48, B81 and P100 samples contain calcite probably related to secondary crystallization processes as observed in petrographic analysis.

**Table 2.** Mineralogical composition (relative abundances of phases were estimated on the basis of the intensity of reflections in the diffraction patterns) of the ceramic body detected by XRD. Legend: Qtz = quartz; Feld= Feldspar; Hem = hematite; Cal = calcite; Di = diopside; CM = total clay minerals.  
 +++++ = very abundant; +++ = abundant; ++ = common; + = scarce.

Sample	Qtz	Feld	Hem	Cal	Di	CM
L11	++++	+	+	+	+	+
PE46	++++	+	+		++	+
CV48	+++	+	+	+	+	+
B81	+++	++	+	+	+	+
CB96	++++	++	++		+	+
P100	++++	+	++	+	++	+
O115	++++	++	++		++	+

**SEM-EDS Analysis**

Morphological analyses by SEM point out the compactness, high degree of vitrification of the black gloss and the clear-cut contact with the ceramic body in all the samples. The gloss thickness is quite uniform and does not exceed 20µm, coherently with the sizes of the slips dated back to III – IV sec. B.C. in the Southern Italy and precisely in the Locrian area [11] (Fig. 3).

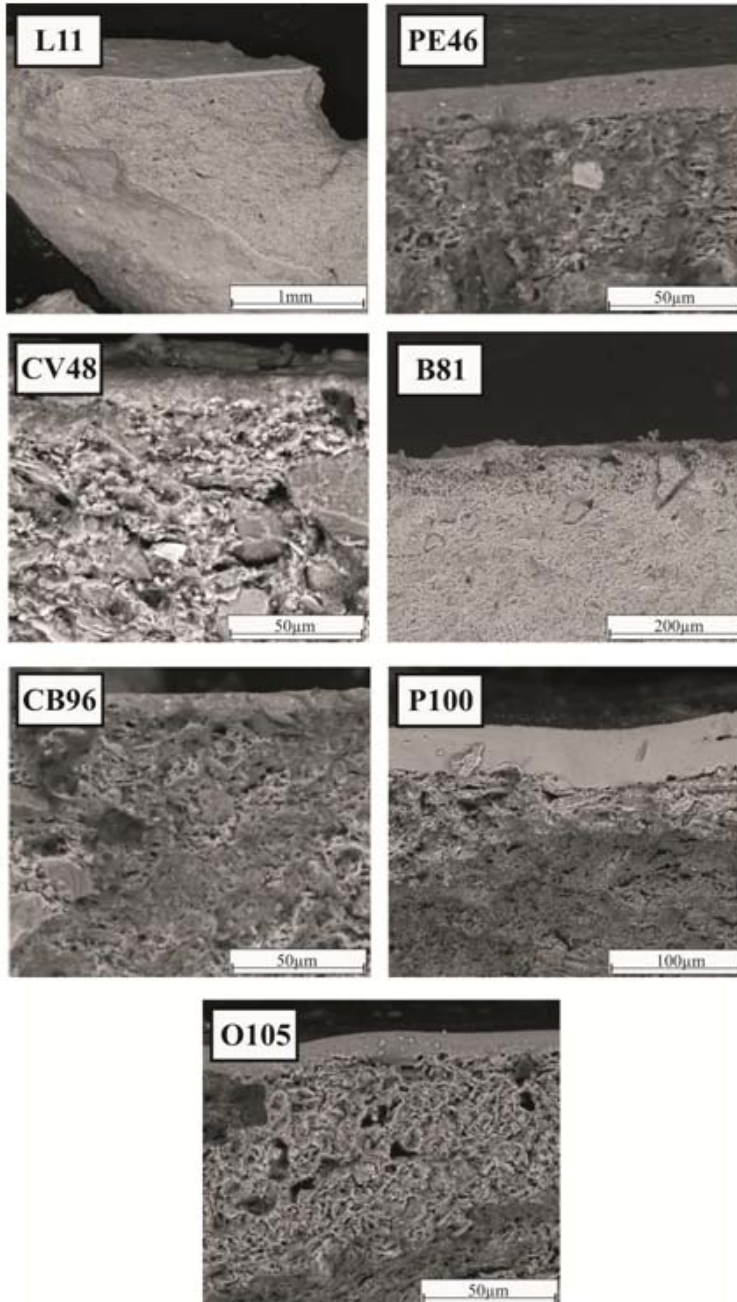


**Fig. 3.** BSE-SEM (Back Scattered Electron) microphotographs with details of ceramic body and gloss

Chemical composition of ceramic body and gloss was achieved by quantitative EDS (Table 3).

The content of Na<sub>2</sub>O varies between about 1-2wt% both in the ceramic body and gloss. MgO ranges among 2-5wt% in ceramic body and 2-3wt% in gloss. Al<sub>2</sub>O<sub>3</sub> reaches values of 10-15wt% in the ceramic body and increases until 26wt% in the slip. The concentrations are different in L11 where the Al<sub>2</sub>O<sub>3</sub> is about of 24% in the ceramic body and 14% in the gloss. SiO<sub>2</sub> amount is about 52-54wt% in the ceramic body and decrease in gloss until 44%; it remains about at 52% only in L11 and P100. K<sub>2</sub>O is about 2-3wt% in ceramic body and about 4-7% in slip, except in L11 and P100 gloss where it is constant at ~2wt%. CaO amount in the ceramic body ranges among 15-21wt% in all samples, whereas it is nearly 1% in L11; in the gloss, CaO decrease until values between 1-9 wt%, only in P100 it remains at ~14wt%. Fe<sub>2</sub>O<sub>3</sub> varies among 6-8wt% in the body and 9-17wt% in the gloss. TiO<sub>2</sub> is nearly 1wt% in both the components.

The samples PE46, CV48, B81, CB96, O115 report similar trends related both to the composition and the variation of oxides wt% between the body and the gloss. In the samples, Si/Al ratios is close to 2 and various amounts of different basic cations in both portions are present, so the dominance of 2:1 phyllosilicate clays can be supposed [15]. A general increase of Al<sub>2</sub>O<sub>3</sub> and Fe<sub>2</sub>O<sub>3</sub> was observed in the slip rather than the ceramic body, on the contrary SiO<sub>2</sub>, CaO and MgO decrease. About raw materials, EDS data suggest how ceramic body is characterized by a clay with good percentage of CaO, whereas the gloss mainly by an illitic type, as the dominance of K among basic cations underlines; in particular the amount of K<sub>2</sub>O seems to double commonly from the ceramic body to the slip.

L11 and P100 achieved results indicating different trends respect to the other samples. There is no clear compositional difference between ceramic body and gloss. In addition, the trends relative to Al<sub>2</sub>O<sub>3</sub> and CaO in L11 gloss seem to be in contrast with the all previous samples: Al<sub>2</sub>O<sub>3</sub> amount decrease, whereas CaO increases.

**Table 3.** Summary of pottery EDS analyses (wt%)

Sample		Na <sub>2</sub> O	MgO	Al <sub>2</sub> O <sub>3</sub>	SiO <sub>2</sub>	K <sub>2</sub> O	CaO	Fe <sub>2</sub> O <sub>3</sub>	TiO <sub>2</sub>
<b>L11</b>	Ceramic body	0.54	2.17	24.9	55.2	2.57	1.41	12.4	0.81
	Gloss	1.60	3.44	14.2	55.6	2.76	9.05	12.30	1.05
<b>PE46</b>	Ceramic body	2.46	5.01	10.1	54.3	2.06	15.23	6.54	4.30
	Gloss	1.09	2.88	25.9	44.3	5.68	1.71	16.9	1.54
<b>CV48</b>	Ceramic body	1.31	4.96	10.2	53.0	3.23	19.9	6.89	0.51
	Gloss	1.84	3.77	18.4	49.5	6.87	6.32	12.30	1.00
<b>B81</b>	Ceramic body	1.17	4.31	10.9	54.8	3.05	18.39	6.42	0.96
	Gloss	2.39	2.66	23.4	44.7	7.08	9.53	9.29	0.95
<b>CB96</b>	Ceramic body	1.04	3.83	10.2	52.5	2.58	21.8	7.32	0.73
	Gloss	2.13	2.85	24.5	49.2	4.27	2.70	13.43	0.92
<b>P100</b>	Ceramic body	1.11	2.61	16.9	52.0	2.95	14.8	8.24	1.39
	Gloss	1.45	2.92	16.2	52.5	2.60	14.86	8.14	1.33
<b>O115</b>	Ceramic body	1.97	3.58	10.2	54.31	2.35	17.69	8.79	1.11
	Gloss	2.47	2.40	26.4	46.64	7.56	1.34	12.4	0.79

**FT-IR analysis**

Sample P100 was undergone to FT-IR analysis to understand the composition of a transparent coating in some portions of the surface.

Infrared spectra of the gloss exhibited the characteristic absorption peaks of PVAc (polyvinyl acetate) centered at 1225, 1120, and 1018cm<sup>-1</sup>, as well as the distinctive signatures of C-H stretching and bending vibrations at 2973, 2926, and at 1433 and 1370cm<sup>-1</sup>, respectively (Fig.4).

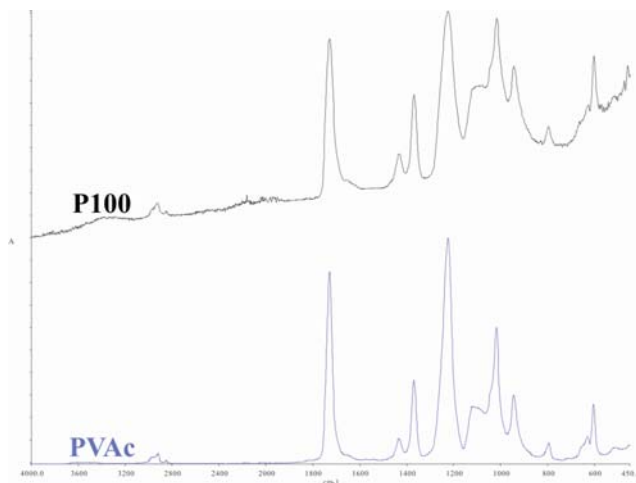


Fig.4. FT-IR spectrum of P100 compared with PVAc (polyvinyl acetate)

## Discussion

The compared evaluation of the results obtained by the different methodologies provided important information about the characterization of the potteries analyzed and their probable authenticity.

The optical microscopy suggests how every sample shows different textural features, although the minerals identified are quite similar.

The XRD analysis allowed to estimate the firing temperature reached by the potteries: the occurrence of diopside ( $\text{CaMgSi}_2\text{O}_6$ ) as neoformation phase in all samples suggests that the original calcareous clay was fired at temperatures higher than  $850^\circ\text{C}$  [14, 16].

SEM-EDS analysis achieved results able to determine the probable authenticity of the potteries studied. In particular, the composition of ceramic body and gloss supplied by microanalysis on PE46, CV48, B81, CB96, O115 and the oxides variation between the two components are coherent with the ancient recipes reported in literature about Magna Graecia potteries. Precisely, the potteries coming from the Magna Graecia analyzed in [6, 11, 17], show content of the major elements, and consequently, compositional trends comparable with these samples. In fact, in the samples studied and in the potteries reported in literature, the different clays in ceramic body and gloss reflects a lower content of silicon, calcium and magnesium and a higher amount of aluminium, iron and potassium in the slip with respect to the body. This decrease of silicon and calcium is related at the minor presence of quartz and carbonate grains in the gloss to allow vitrification in a shorter time and at a lower temperature than those needed for the body clay [11].

On the contrary, EDS analysis on L11 and P100 samples points out incongruences in the compositional trends with the traditional technological processes cited previously. In fact ceramic body and gloss present similar compositions without any clear variations in the oxides content, how instead in the other samples. Moreover especially L11 shows amounts in oxides, i.e.  $\text{SiO}_2$ ,  $\text{Al}_2\text{O}_3$ ,  $\text{K}_2\text{O}$ ,  $\text{CaO}$ ,  $\text{Fe}_2\text{O}_3$  beyond the compositional ranges characterizing PE46, CV48, B81, CB96 and O115.

The FT-IR analysis carried out on surface of P100 indicated clearly the presence of PVAc (polyvinyl acetate) a common synthetic polymer used nowadays. The hypothesis of its application as a restoration work was excluded because the *Phiale* is perfectly intact without any trace of fractures or other kind of damages; probably the polymer was applied simply such



as a rough coating. This result is a further element doubting the authenticity of the sample P100 (Fig. 4).

## Conclusions

The work demonstrated the validity of a complementary use of different analytical techniques for an archaeometric investigation aimed both to the characterization and the evaluation of the authenticity of ceramic artefacts. The interpretation and comparison of petrographic, SEM-EDS, XRD and FT-IR data allowed defining the technological processes characterizing seven red and black-figured potteries seized from a unknown location between Sicily and Calabria. In particular EDS results discriminate two types of samples: the first one constituted by PE46, CV48, B81, CB96, O115 and the second one by L11 and P100. The first group was produced according to the ancient recipes used in Magna Graecia area and indicated in literature: i.e. with defined compositional ranges in terms of major elements and with specified variations of the oxides amounts between ceramic body and gloss. So these artefacts are probably authentic.

The contents of elements and their variations among body and slip in L11 and P100 do not reflect the trends cited previously. About L11, there are no clear evidences about the authenticity: the different productive process could be a clue, but it could be related simply also to another area or period of production. So in this regard, more analysis would be requested. On the other side, in P100, the identification of polyvinyl acetate such as possible rough coating and not as restoration work supports the hypothesis of non-authenticity of the sample.

## References

- [1] G.M. Crisci, M.F. La Russa, M. Macchione, M. Malagodi, A.M. Palermo, S.A. Ruffolo, *Study of archaeological underwater finds: deterioration and conservation*, **Applied Physics A**, **100**(3), 2010, pp. 855-863.
- [2] P. Aloise, M. Ricca, M.F. La Russa, S.A. Ruffolo, C.M. Belfiore, G. Padeletti, G.M. Crisci, *Diagnostic analysis of stone materials from underwater excavations: the case study of the Roman archaeological site of Baia (Naples, Italy)*". **Applied Physics A**, **114**(3) 2014, pp. 655-662.
- [3] C.M. Belfiore, M.F. La Russa, D. Barca, G. Galli, A. Pezzino, S.A. Ruffolo, M. Viccaro, G.V. Fichera, *A trace element study for the provenance attribution of ceramic artefacts: the case of Dressel 1 amphorae from a late-Republican ship*, **Journal of Archaeological Science**, **43**, 2014, pp. 91-104.
- [4] C.M. Belfiore, M.F. La Russa, L. Randazzo, G. Montana, A. Pezzino, S.A. Ruffolo, Aloise P. *Laboratory tests addressed to realize customized restoration procedures of underwater archaeological ceramic finds*, **Applied Physics A**, **114**(3), 2014, pp. 741-752.
- [5] M. Ricca, V. Comite, M.F. La Russa, D. Barca, *Diagnostic analysis of bricks from the underwater archaeological site of Baia (Naples, Italy): preliminary results*, **Rendiconti Online della Società Geologica Italiana**, **38**, 2016, pp. 85-88.
- [6] D. Barca, M.F. La Russa, G.M. Crisci, *Technological and geochemical study of two red-figured vases of unknown provenance by various analytical techniques*, **Applied Physics A**, **100**(3), 2010, pp. 911-917.
- [7] U. Hofmann, *Die chemischen Grundlagen der griechischen Vasenmalerei*, **Angewandte Chemie**, **74**, 1962, pp. 397-406.
- [8] M. S. Tite, M. Bimson, I.C. Freestone, *An examination of the high gloss surface finishes on Greek Attic and Roman Samian wares*. **Archaeometry**, **24**, 1982, pp. 117-126.
- [9] J.V. Noble, **The Techniques of Painted Attic Pottery**, Watson-Guptill, New York, 1988.

- [10] P. Mirti, *X-ray microanalysis discloses the secrets of ancient Greek and Roman potters*, **X-ray Spectrom**, **29**, 2000, pp. 63-72.
- [11] P. Mirti, M. Gulmini, A. Perardi, P. Davit, D. Elia, *Technology of production of red figure pottery from Attic and southern Italian workshops*, **Analytical and Bioanalytical Chemistry**, **380** (4), 2004, pp. 712-718.
- [12] Y. Maniatis, E. Aloupi, A.D. Stalios, *New evidence for the nature of the Attic black gloss*, **Archaeometry**, **35**, 1993, pp. 23-34.
- [13] I.K. Whitbread, **Greek Transport Amphorae. A Petrological and Archaeological Study**, Athens, 1995, p.146.
- [14] G. Cultrone, C. Rodriguez-Navarro, E. Sebastian, O. Cazalla, M. J. De La Torre, *Carbonate and silicate phase reactions during ceramic firing*, **European Journal of Mineralogy**, **13**, 2001, pp. 621-634.
- [15] I. Sandu, V. Cotiuga, A.V. Sandu, A.C. Ciocan, G.I. Olteanu, V. Vasilache, *New archaeometric characteristics for ancient pottery identification*, **International Journal of Conservation Science**, **1**(2), 2010, pp. 75-82.
- [16] M. P. Riccardi, B. Messiga, P. Duminuco, *An approach to the dynamics of clay firing*, **Applied Clay Science**, **15**, 1999, pp. 393-409.
- [17] P. Mirti, L. Appolonia, A. Casoli, *Technological features of Roman terra sigillata from Gallic and Italian centres of production*, **Journal of Archaeological Science**, **26**(12) 1999, pp. 1427-1435.

---

*Received: August, 14, 2016*

*Accepted: September, 25, 2016*